International Journal of Mechanical Sciences 84 (2014) 61–72

Contents lists available at ScienceDirect

International Journal of Mechanical Sciences

journal homepage: www.elsevier.com/locate/ijmecsci

Sandwich plates with functionally graded metallic foam cores subjected to air blast loading

X.R. Liu [a], X.G. Tian [a,*], T.J. Lu [a,*], B. Liang [b]

[a] State Key Laboratory for Mechanical Structural Strength and Vibration, Xi'an Jiaotong University, Xi'an 710049, China
[b] Xuhai College, China University of Mining & Technology, Xuzhou 221008, China

ARTICLE INFO

Article history:
Received 16 January 2013
Received in revised form
9 July 2013
Accepted 20 March 2014
Available online 29 March 2014

Keywords:
Sandwich plate
Functionally graded material
Aluminum foam
Air blast
Finite element

ABSTRACT

The dynamic responses and blast resistance of all-metallic sandwich plates with functionally graded close-celled aluminum foam cores are investigated using finite element simulations, and compared with those of ungraded single-layer sandwich plates. Upon validating the numerical approach using existing experimental data and introducing the present computational model, different graded sandwich plates under air blast loading are analyzed in terms of deformation and blast resistance. The effects of face-sheet arrangements and interfacial adhesion strength between different foam layers are quantified. The results demonstrate that relative to conventional ungraded plates subjected to identical air blast loading, the graded plates possess smaller central transverse deflection and superior blast resistance, with further improvement achievable by optimizing the foam core arrangement. The blast resistance of both graded and ungraded sandwich plates subjected to the constraint of equivalent mass is also explored.

1. Introduction

Lightweight all-metallic sandwich plates consisting of two thin and strong face-sheets separated by thick and weak cellular cores have been increasingly exploited as blast resistant structures [1–9]. The face-sheets are typically made of high strength solid material whilst the cellular metallic cores are highly porous, such as metallic foams with random cell topologies and periodically arranged lattice structures (e.g., honeycombs, pyramidal trusses and prismatic corrugations). When subjected to impulsive loading, it has been established that the cellular core enables large plastic deformation and hence absorbs a large amount of impact energy, contributing to the superior blast resistance of the sandwich structure relative to monolithic counterpart with equivalent mass [10–16].

Radford et al. [17] utilized the metallic foam projectile to successfully simulate the high intensity pressure impulse exposed on sandwich structures, with the applied pressure versus time impulse having a peak pressure on the order of 100 MPa and loading time of approximate 100 μs. This experimental technique was subsequently employed by Radford et al. [18,19], McShane et al. [20] and Tagarielli et al. [21] to investigate the shock resistance of clamped sandwich beams/plates having lattice truss or metallic foam cores, revealing that the sandwich structures have superior shock resistance compared to monolithic counterparts. Bahei-El-Din et al. [22] proposed a modified sandwich plate design, with a thin polyurea interlayer inserted between the outer face-sheet (loaded side) and the foam core. The simulation results showed that, under blast loading, the modified sandwich plate reduced foam core crushing, face-sheet strain and overall deformation relative to conventional sandwich design, absorbing however also less energy. Zhu et al. [23–25] performed air blast experiment and finite element (FE) simulation on aluminum foam-cored sandwich panels. The simulation results well captured the deformation patterns of the sandwich panels observed in the tests, and agreed with experimental measurements. Nurick et al. [26], Karagiozova et al. [27] and Theobald et al. [28] investigated the responses of sandwich panels subjected to intense air blast loading both experimentally and numerically, and found that the face-sheet thickness affects significantly the blast resistance of sandwich panels; the compromise between improved energy absorption and loading transfer through the core to the bottom face-sheet was also explored. Shen et al. [29] implemented blast loading tests on curved sandwich panels using a four-cable ballistic pendulum with corresponding sensors. It was demonstrated that, due to the initial curvature, the performance of sandwich shells is superior to that of equivalent mass solid counterparts and flat sandwich panels. Existing theoretical and experimental studies also demonstrate that, broadly speaking, the

* Corresponding authors. Tel./fax: +86 29 8266 8751.
E-mail addresses: tiansu@mail.xjtu.edu.cn (X.G. Tian), tjlu@mail.xjtu.edu.cn (T.J. Lu).

http://dx.doi.org/10.1016/j.ijmecsci.2014.03.021
0020-7403/

dynamic responses of sandwich structures subjected to air (or underwater) explosion may be split into three sequential stages: (1) fluid–structure interaction, (2) core compression, and (3) structure bending and stretching.

Since the material characteristics of layered materials can be controlled in a predetermined way, a growing number of theoretical and experimental studies focused on how sandwich structures with graded cores perform under impulsive loading. For typical instance, Li et al. [30] found that the choice of layer gradation significantly affects the impulse response of layered and graded metal–ceramic composites. Regarding low velocity impact responses of sandwich structures having functionally graded cores, Apetre et al. [31] demonstrated that the functionally graded core reduces the maximum strain and can be used effectively to mitigate or completely prevent impact damage. Utilizing three-dimensional (3D) finite element (FE) simulations, Etemadi et al. [32] demonstrated that sandwich beams with functionally graded cores exhibited increasing maximum contact force and decreasing maximum strain in comparison with those having homogenous cores. For sandwich plates with multilayered graded foam cores, Wang et al. [33] demonstrated experimentally with a shock tube facility that different core configurations led to considerably different dynamic responses, due mainly to different degrees of deformation and failure. Chittineni and Woldesenbet [34] experimentally investigated the quasi-static compression performance of four-layer functionally graded composites fabricated from four different hollow particles, and found that the arrangement of layers affected significantly the compressive strength and energy absorption of the composite. The shock behavior of functionally graded circular plates with peripherally clamped boundaries under a drop-weight was numerically simulated by Gunes and Aydin [35]. Whilst compositional gradient exponent, impact velocity and plate radius were found to influence significantly the impact response of the plate, the layer number through the plate thickness had a minor effect. Ajdari et al. [36] investigated using finite element models the dynamic crushing and energy absorption of two-dimensional (2D) honeycombs with functionally graded density. It was shown that decreasing the relative density in the direction of crushing can enhance the energy absorption capability of the honeycomb at early stages of crushing. Employing the same experimental device of Wang et al. [33], Gardner et al. [37] investigated the performance of functionally graded sandwich composite beams. It was found that increasing the layer number of monotonically graded foam core helped to maintain the structural integrity and enhanced the blast resistance of the sandwich composite, because acoustic wave impedance mismatch between successive layers was decreased.

Despite extensive theoretical and experimental investigations as discussed above on sandwich structures subjected to air blast loading, at present there is yet a systematic study focusing on the dynamic responses and blast resistance of sandwich configurations with graded metallic foam cores. With 3D FE simulations, this deficiency is addressed in the present work by studying the air blast behavior of sandwich plates with multilayered graded aluminum foam cores. The influences of simulated pressure history (rectangular versus exponential type), foam core layer number and interfacial connection strength are considered. For comparison, conventional single-layer sandwich plates with homogeneous aluminum foam cores are also computed. The paper is organized in the following manner. In Section 2, the numerical approach is validated by comparing with existing experimental measurements for both circular and square plates [19,23]. Computational models for both conventional and graded sandwich plates are introduced in Section 3. Section 4 presents and analyzes the simulation results considering two different joint connection types, with particular focus placed upon the influence of core layer number and core layer arrangement on blast resistance. Section 5 examines the influence of face-sheet arrangements on the dynamic responses of sandwich plates, whilst Section 6 illustrates the blast resistance of sandwich plates with equivalent mass and compares with the case of equivalent volume. At last, the conclusions are drawn in Section 7.

2. Validation of numerical approach

2.1. Validation with circular plates

Numerical simulations are performed using the commercially available FE code LS-DYNA 971. For validation, the responses of circular metallic aluminum foam-cored sandwich plates tested by Radford et al. [19] to simulated blast loading are numerically predicted. The sandwich plates (denoted here as S) consist of two identical AISI 304 stainless steel face-sheets (1.18 mm in thickness) and close-celled aluminum foam (Alporas) core having 15.9% relative density and 10 mm core height. Circular monolithic stainless steel plates (denoted here as M) having the same mass as the sandwich plates are also simulated. Both the sandwich and monolithic plates have an in-plane radius of 80 mm and are peripherally fully clamped. The blast loading is generated by cylindrical aluminum foam projectiles of diameter 28.5 mm, impacting at the central circular area of the top face. As previously mentioned, it has been established that metallic foam projectiles can be used to create pressure impulses exposed on sandwich structures, with peak pressure on the order of 100 MPa and loading time of approximately 100 μs [17]. The performance of each plate is quantified by permanent transverse deflection at the center of the bottom face, which is experimentally measured [19]. For each type of plate, Table 1 summarizes the impulse/area exerted on the plate by aluminum foam projectile and the corresponding central deflection of the bottom face measured experimentally [19]. Accordingly, in the present study, $\sim$10 kN s m^{-2} is selected as the impulse/area for all FE simulations, mimicking a pressure magnitude of about 100 MPa.

For numerical simulations, the air blast loading is modeled as pressure versus time history and is applied to the top face of the plate over a central circular region of diameter 28.5 mm. Two different pressure histories, rectangular and exponential, are adopted. For the rectangular case, the pressure versus time history has a time duration of 100 μs, and the plateau pressure is derived from the impulse/area (as listed in Table 1) based on impulse conservation. For example, the impulse/area exerted on sandwich plate S2 is 13.31 kN s m^{-2}, while the corresponding pressure is 133.1 MPa, as shown in Fig. 1a. For the exponential case, the applied pressure is described by exponentially decaying time-dependent history, as

$$p(t) = p_0 e^{-t/t_0} \tag{1}$$

where p_0 is the peak pressure and t_0 is the time taken by the shock wave to decay to $1/e$ of the peak pressure. In this case, the

Table 1
Impulse/area and the corresponding central deflection of bottom face for both sandwich plates (S) and monolithic plates (M) [19].

Specimen	Impulse/area (kN s m^{-2})	Central deflection of bottom face (mm)
S1	9.93	8.1
S2	13.31	12.8
M1	10.51	10.6
M2	11.75	12.2
M3	13.07	14.2

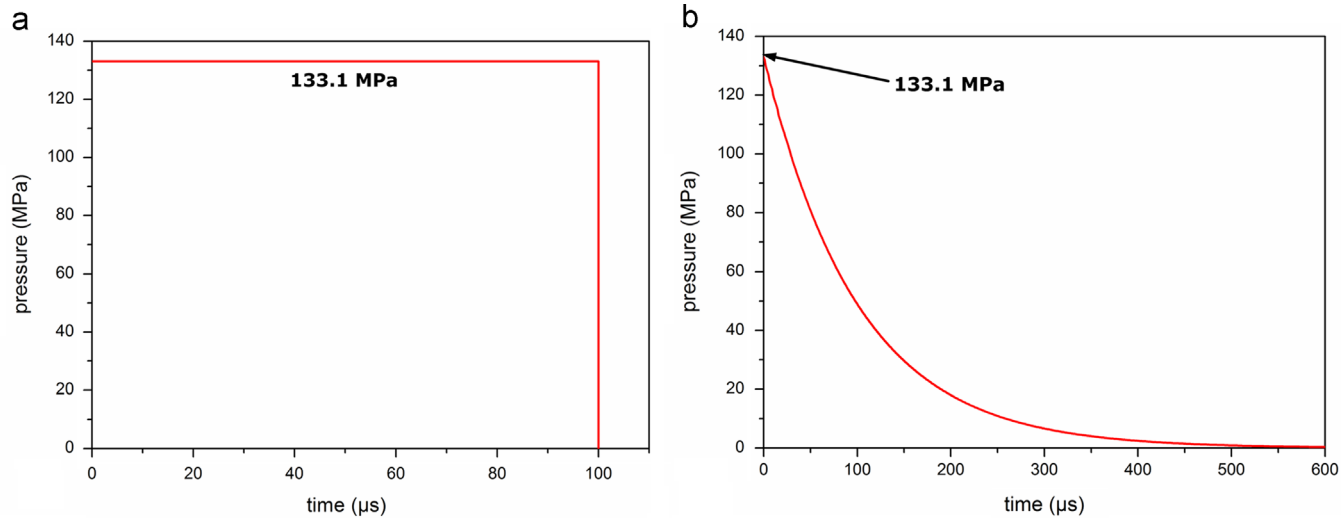

Fig. 1. Pressure versus time history exerted on top face-sheet of sandwich plate S2: (a) rectangular shape and (b) exponential shape.

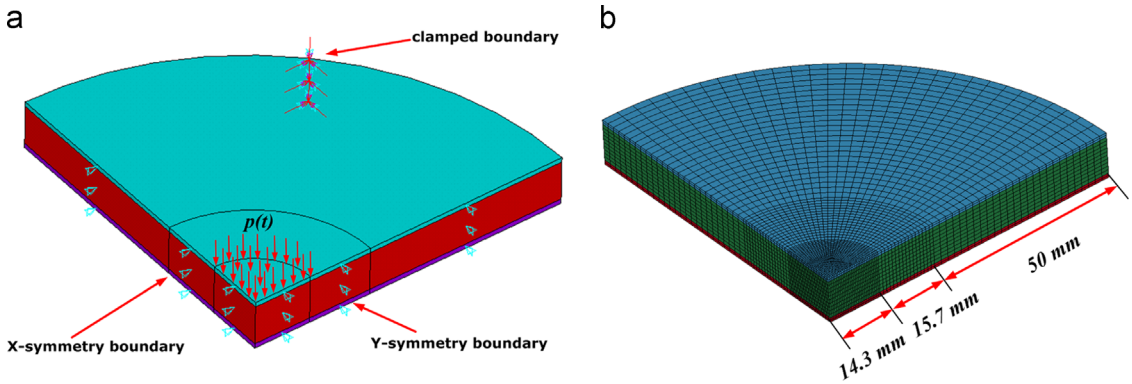

Fig. 2. A quarter of sandwich plate: (a) boundary conditions and (b) FE model.

impulse/area loaded on the top face (I) is

$$I = p_0 t_0 \tag{2}$$

Here, the time constant is specified as $t_0 = 100$ μs whilst the peak pressure p_0 is identical to the plateau pressure of the rectangular case, as shown in Fig. 1b for S2. Consequently, the two pressure histories have the same loading criterion on the basis of impulse conservation.

Due to symmetry, only a quarter of the circular sandwich plate is simulated, with symmetrical boundary conditions imposed (X-symmetry boundary and Y-symmetry boundary, see Fig. 2a). Besides, fully clamped boundary condition is prescribed on the perimeter of the plate. The sandwich plate is modeled using eight-node linear solid elements with reduced integration. As shown in Fig. 2b, three segments having different mesh densities and dimensions in the radial direction are divided for all the components of sandwich plate. For the inner segment, there are 30 brick elements in the radial direction, each element about 0.5 mm in size. For the middle and outer segments, the element size is approximately 1 mm and 2 mm, respectively. The inner segment has smaller elements as the loading impulse is applied in this region. In the thickness direction, both the top and bottom face-sheets are meshed with two elements, each having a size of about 0.5 mm; the element size across the foam core is fixed at 1 mm so that there are 10 elements in total. Correspondingly, monolithic plates are simulated using identical boundary conditions and element meshing in the radial direction, with element size in the thickness direction about 0.5 mm. Upon ensuring numerical convergence, the total number of elements selected for the sandwich plates is 27,090 whilst that for the monolithic plates is 11,610.

The mechanical behavior of AISI 304 stainless steel is described using the plastic kinematic constitutive model (MAT_PLASTIC_KINEMATIC), which is a bi-linear elasto-plastic constitutive relationship with two choices of hardening formulations (isotropic or kinematic). The strain rate sensitivity is taken into account with the Cowper–Symonds model, as

$$\frac{\sigma_d}{\sigma_Y} = 1 + \left(\frac{\dot{\varepsilon}}{C}\right)^{(1/P)} \tag{3}$$

where σ_d is the dynamic yield stress, σ_Y is the yield stress, $\dot{\varepsilon}$ is the strain rate, C and P are dynamic material constants. The material parameters for AISI 304 stainless steel are: mass density $\rho = 8060$ kg/m^3, Young's modulus $E = 210$ GPa, Poisson ratio $\upsilon = 0.3$, yield stress $\sigma_Y = 300$ MPa, tangent modulus $E_t = 1.7$ GPa, $C = 10^6$ s^{-1} and $P = 9$. The values of C and P are derived from Radford et al. [19].

The close-celled aluminum foam of relative density 15.9% is modeled using a honeycomb type constitutive model (MAT_HONEYCOMB), which has the ability to simulate the mechanical behavior of metallic foams under both static and dynamic loadings. The quasi-static compressive stress versus strain curve of the aluminum foam is taken directly from Radford et al. [19]. As the relative density of the foam is relatively low, it may be taken

as strain rate insensitive according to the studies of Zhang et al. [38,39].

With exponential shape pressure history (Fig. 1b) selected, the predicted time history of the central transverse deflection for sandwich (S2) and monolithic (M3) plates subjected to13 kN s m^{-2} impulse/area is plotted in Fig. 3. The bottom face of the sandwich plate has significantly smaller transverse deflection relative to that of its monolithic counterpart, demonstrating the superiority of the sandwich plate, which is consistent with the experimental result presented in Radford et al. [19].

Fig. 4a presents the representative transverse displacement contours of sandwich plate S2 at 2000 μs. The greatest transverse displacement occurs at the central area of the plate, in conformity with experimental observation [19]. For both types of pressure history (see Fig. 1), Fig. 4b compares the numerical predictions with the experimental measurements of Radford et al. [19]. The rectangular pressure history is seen to substantially over-predict the experimental measurements, whilst the exponential pressure history leads to reasonable agreement between experiment and FE simulation. Using rectangular pressure history, Radford et al. [19] also found that their FE simulation results over-predict, although they did not consider the exponential pressure history. Consequently, the exponential pressure history is employed in all subsequent FE simulations.

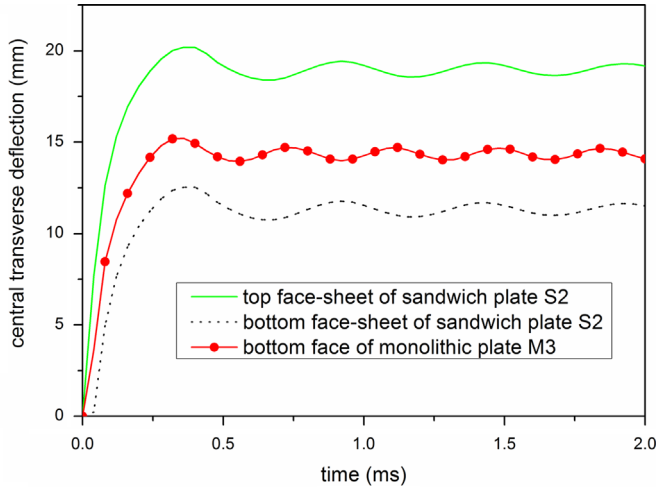

Fig. 3. Predicted time history of central transverse deflection for sandwich (S2) and monolithic (M3) plates subjected to 13 kN s m^{-2} impulse/area using exponential shape pressure history.

2.2. Validation with square plates

To validate the numerical approach, aluminum foam-cored sandwich plates tested by Zhu et al. [23] under air blast loading are simulated. The specimens consist of two identical aluminum alloy (2024-T3) face-sheets and an aluminum foam core with 6% relative density. The peripherally fully clamped sandwich plates have in-plane dimensions of 250 mm × 250 mm, whilst the face-sheet thickness and foam core height are varied according to those specified in Table 2. The air blast loading is applied to the top face-sheet uniformly (pressure history of exponential shape with t_0=100 μs) and the blast resistance of each sandwich is quantified by the permanent transverse deflection at the center of the bottom face-sheet, which are experimentally measured (Table 2) [23].

For FE simulation, only a quarter of the sandwich plate is analyzed due to symmetry, with symmetrical boundary conditions imposed (Fig. 9a). In addition, fully clamped boundary conditions are applied to the periphery of the plate. The sandwich plate is modeled using eight-node linear solid elements with reduced integration as shown in Fig. 9b. To ensure numerical convergence, the number of elements selected for the sandwich plate is 55,000.

The mechanical behavior of aluminum alloy 2024-T3 (mass density 2680 kg/m^3, Young's modulus 72 GPa, Poisson ratio 0.33, yield stress 318 MPa and tangent modulus 737 MPa) is governed by material model MAT_PLASTIC_KINEMATIC. The strain rate sensitivity of 2024-T3 is low and hence neglected in the simulation.

Table 2
Specifications of foam-cored sandwich plates and experimental results [23].

No. of specimen	Face-sheet thickness (mm)	Core thickness (mm)	Impulse (Ns)	Central deflection of bottom face-sheet (mm)
1	1.0	20	18.29	4.9
2	1.0	20	22.57	6.1
3	0.8	30	22.67	6.2
4	1.0	30	22.32	5.6
5	1.0	30	25.85	7.0

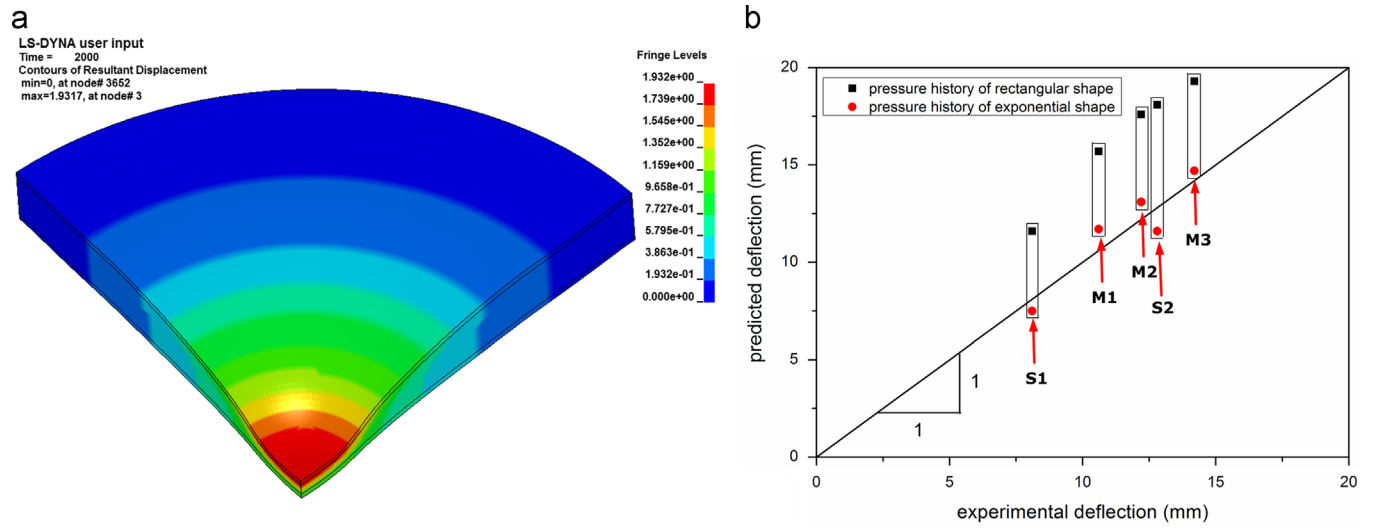

Fig. 4. (a) Transverse displacement contours of sandwich plate S2 (Table 1) at 2000 μs; (b) comparison between experimentally measured and numerically predicted central transverse deflection of bottom face.

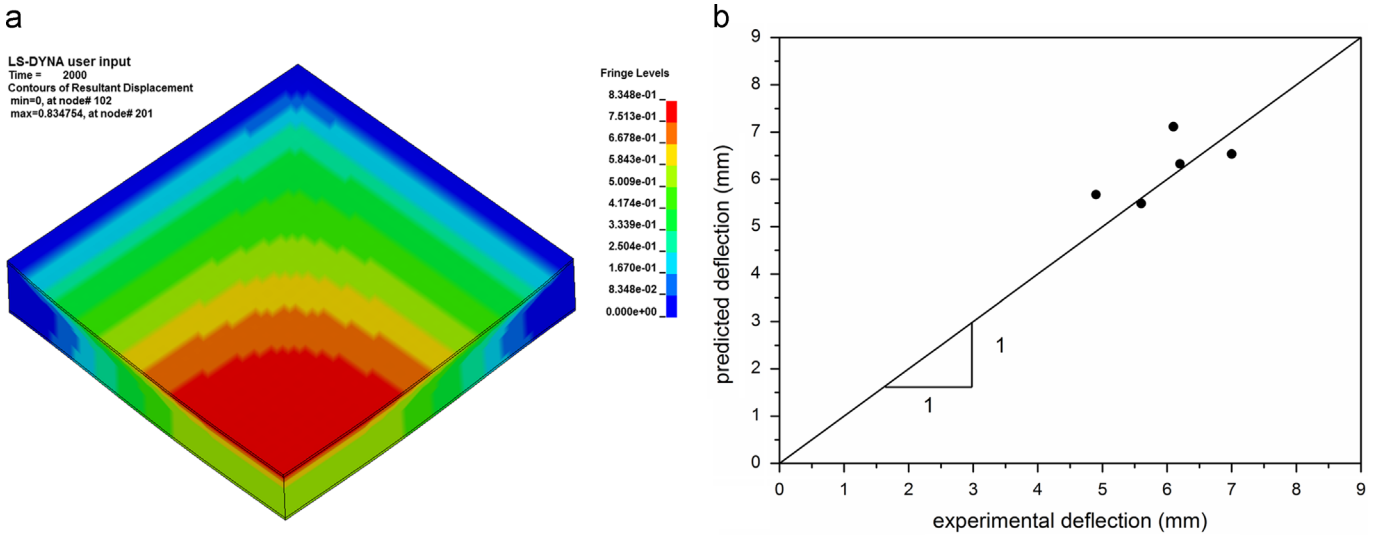

Fig. 5. (a) Transverse displacement contours of aluminum foam-cored sandwich specimen 1 (Table 2) at 2000 μs; (b) comparison between experimentally measured and numerically predicted central transverse deflection of bottom face-sheet.

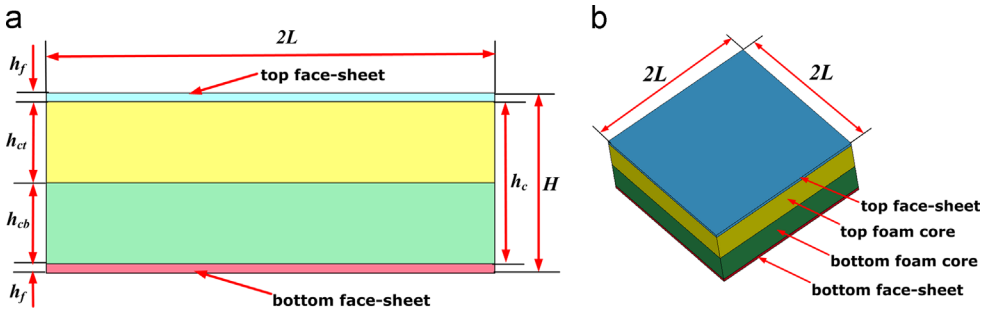

Fig. 6. Sandwich plate with the two-layer graded aluminum foam core: (a) side view and (b) overall view.

The close-celled aluminum foam with 6% relative density is simulated using a honeycomb constitutive model (MAT_HONEYCOMB). The quasi-static compressive stress versus strain curve is taken from Zhu et al. [23] As the relative density of the foam is relatively low, according to the experimental and theoretical studies of Zhang et al. [38,39], it may be taken as strain rate insensitive.

Fig. 5a shows the transverse displacement contours of specimen 1 (Table 2) at 2000 μs. The sandwich plate has the greatest transverse displacement at the central area, comply with experimental observation [23]. Fig. 5b compares the experimental measurements [23] with numerical predictions. It is seen that the points are close to the line of perfect match, suggesting reasonable agreement between experiment and FE simulation.

According to the validation presented above for both circular and square plates, it may be concluded that the present FE simulation procedures can be used to investigate the dynamic responses of metallic aluminum foam-cored sandwich plates under blast loading.

3. Computational model

3.1. Modeling geometry and material property

As shown schematically in Fig. 6, consider next a sandwich plate with a two-layer close-celled aluminum foam core having different relative densities and (for simplicity) identical thickness (i.e., $h_{ct}=h_{cb}$), with total thickness H and length/width $2L$. The top and bottom face-sheets are identical and made of AISI 304 stainless steel, each having thickness h_f. For reference, the conventional sandwich plate has core thickness (h_c) identical to the sum of the two foam layers, $h_c=h_{ct}+h_{cb}$.

The close-celled aluminum foam selected for the present study mimics that manufactured via the foaming route by Southeast University (SEU) of China, which has been studied extensively, both experimentally and theoretically [38,39]. It should be mentioned here that, in terms of cellular topology and mechanical performance, the SEU aluminum foam is similar to the Alporas foam studied by, amongst many others, Radford et al. [18,19], which is also fabricated via the foaming route and commercially available from Shinko Wire Co. Ltd. (Amagasaki, Japan).

In addition to sandwich plates with two-layer foam cores shown in Fig. 6, conventional sandwich plates with ungraded foam cores and sandwich plates having up to six-layer graded foam cores are also considered; see Fig. 7. The relative density of individual foam layers is varied from 10% to 19.7%, denoted sequentially as F1, F2, F3, F4, F5 and F6. For F1 and F6 foam layers, the experimentally measured compressive stress versus strain curves are plotted in Fig. 8. For simplicity, the corresponding stress versus strain curves for F2, F3, F4 and F5 foam layers are obtained from linear interpolation between F1 and F6, as shown in Fig. 8. Typically, the plateau stress of metallic foams has a power relation with the relative density, as

$$\frac{\sigma_{pl}}{\sigma_s}=\alpha r^{3/2} \tag{4}$$

where σ_{pl} is the plateau stress of metallic foams, σ_s is the yield stress of the parent material, α is a material constant, and r is the

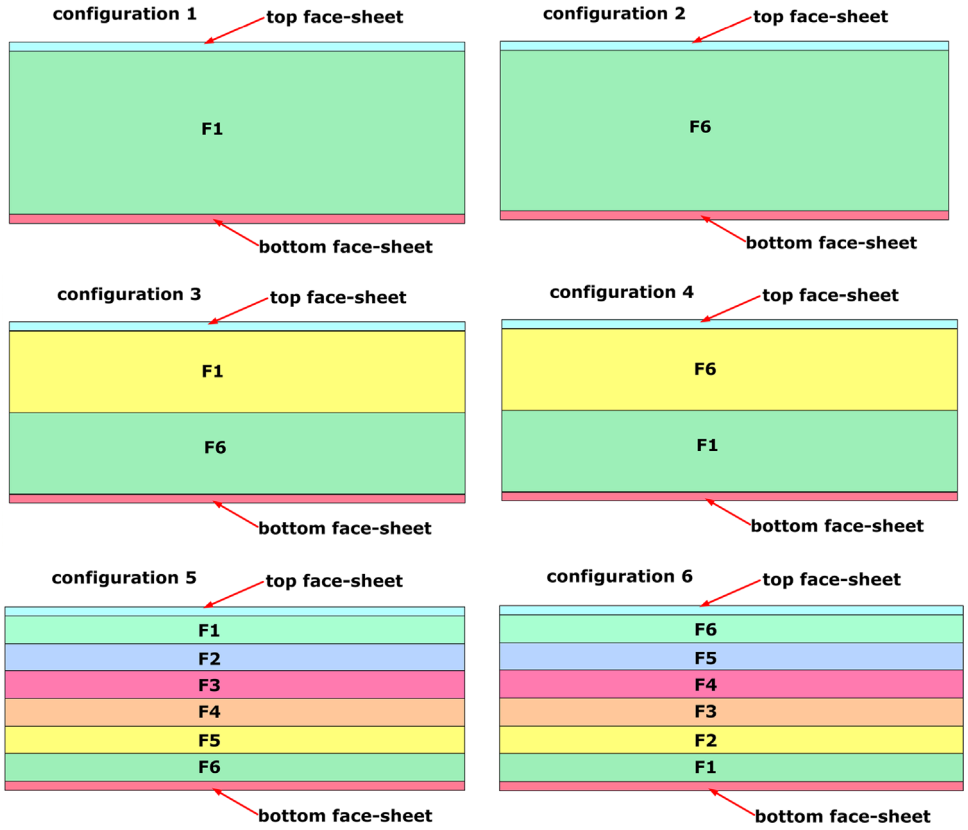

Fig. 7. Schematic illustration of conventional (ungraded) and graded sandwich plates with close-celled aluminum foam cores.

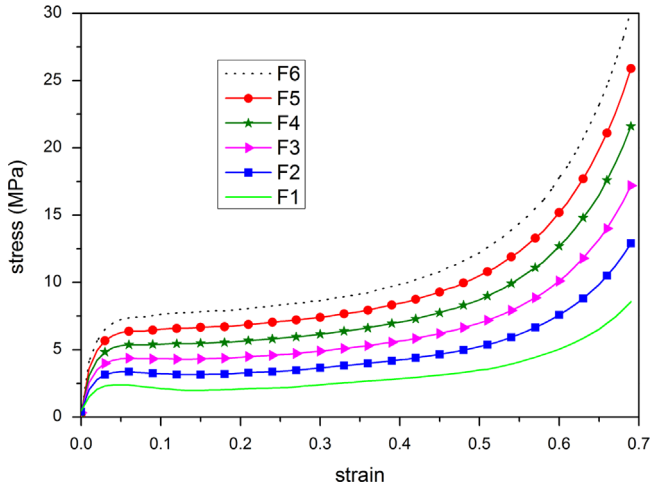

Fig. 8. Uniaxial compressive stress versus strain curves of close-celled aluminum foams: F1 and F6 are obtained from quasi-static uniaxial compression tests whilst F2, F3, F4 and F5 are obtained from linear interpolation between F1 and F6.

foam relative density. Based on the linear interpolation of stress versus strain curve, the relative density of F1, F2, F3, F4, F5 and F6 is obtained as 10%, 12.2%, 14.3%, 16.2%, 18% and 19.7%, respectively.

As shown in Fig. 7, configurations 1 and 2 (conventional sandwich plates) contain single-layer foam cores with relative density F1 and F6, respectively. Regarding the simplest graded sandwich plate containing the two-layer foam core, configuration 3 has the gradation of F1/F6 and configuration 4 has the gradation of F6/F1. In a previous study [40], we found that a graded foam core with relative density increasing from the loaded side to the other side leads to worst blast resistance whilst that with decreasing relative density has the best performance. Therefore, two extreme gradations are used to construct graded sandwich plates considering having more than two foam layers: one has increasing relative density from the top face (loaded side) to the bottom face (other side) and the other has decreasing relative density. As the maximum number of foam layers is constrained by the minimal thickness of foam layer required to retain the material property of close-celled aluminum foam, six-layer graded foam cores are adopted here: configuration 5 has gradation F1/F2/F3/F4/F5/F6 and configuration 6 has gradation F6/F5/F4/F3/F2/F1; see Fig. 7. For both configurations 5 and 6, the overall thickness of the six-layer graded foam core is h_c, with each individual layer having identical thickness $h_c/6$.

The behavior of the AISI 304 stainless steel is simulated using the same approach as previously described in Section 2.1. Close-celled aluminum foams with six relative densities and quasi-static uniaxial compressive stress versus strain curves shown in Fig. 8 are simulated using a honeycomb constitutive model (MAT_HONEYCOMB). Recent experimental and theoretical studies [38,39] reveal that the aluminum foam considered in the present study does not exhibit particularly significant strain rate effect, especially when its relative density is less than about 20%.

3.2. Finite element model

Air blast loading is modeled as uniform pressure (pressure history of exponential shape with $p_0=70$ MPa and $t_0=100$ μs) exposed on the top face of the sandwich plate. Due to symmetry of both the structure and the loading condition, one quarter of the sandwich plate is analyzed. For illustration, Fig. 9a depicts the symmetric boundary conditions imposed upon the graded sandwich plate. In addition, fully clamped boundary conditions are applied to the periphery of the plate.

Eight-node linear solid elements with reduced integration are used to model the sandwich plate. Typically, to ensure numerical

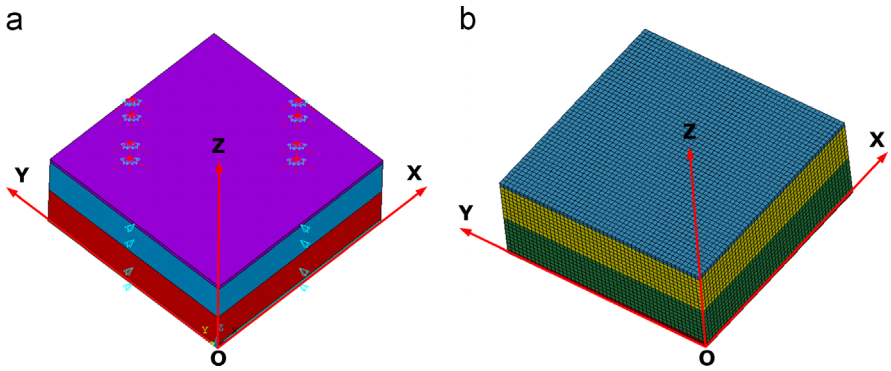

Fig. 9. A quarter of graded sandwich plate: (a) constraint conditions and (b) finite element model.

convergence, the number of elements selected for the sandwich plate is 55,000, as shown in Fig. 9b. The same mesh density is utilized in both X and Y directions for all sub-components of the plate. There are 50 brick elements in both directions, with each element 5 mm in size. In the thickness direction, both the top and bottom faces are meshed with two elements (element size 2.5 mm), while the foam core element has size 5 mm.

4. Results and discussion

Two different types of connection are considered for the sandwich plate: perfect connection and disjointed connection. For perfect connection, the face-sheets and the foam core as well as individual foam layers in the core are glued perfectly, with shared nodes at each interface. For disjointed connection, each part of the sandwich plate is fully disjointed and kept in contact without cohesion, but interpenetration is not allowed. Surface to surface contact algorithm in LS-DYNA 971 is employed at the disjointed interfaces to model this type of connection. Accordingly, the FE simulation results presented in this section include two parts: (1) responses of sandwich plates with perfect connection and (2) responses of sandwich plates with disjointed connection.

Unless otherwise stated, typical geometrical dimensions (Fig. 6) are specified as the following: length/width of sandwich plate $2L=500$ mm, top/bottom face-sheet thickness $h_f=5$ mm, top/bottom foam core thickness $h_{ct}=h_{cb}=45$ mm, overall foam core thickness $h_c=h_{ct}+h_{cb}=90$ mm, total thickness $H=100$ mm. The results are expressed in dimensionless form, with transverse deflection normalized as δ/L and time as $t/(L\sqrt{\rho/\sigma_Y})$.

4.1. Responses of sandwich plates with perfect connection

During the blast event, the shape of the sandwich plate varies from the initially plain profile to a shape with largest transverse deflection at the central region due mainly to foam core compression, as shown in Fig. 10 for the case of a two-layer graded sandwich plate with perfect connection. To present the maximum transverse deflection of the graded sandwich plate, three representative nodes located separately at the center of the top face-sheet (node 2602), the bottom face-sheet (node 7804) and the interface 1 (node 15,607) are selected. However, for conventional and six-layer graded sandwich plates, only two nodes at the center of the top and bottom face-sheets are selected as the representative ones.

Fig. 11a presents the time history of normalized transverse deflection and normalized foam core crushing in the graded sandwich plate of configuration 4. Foam core crushing is defined as the difference between the transverse displacements of two adjacent nodes as shown in Fig. 10. Top foam core crushing, for

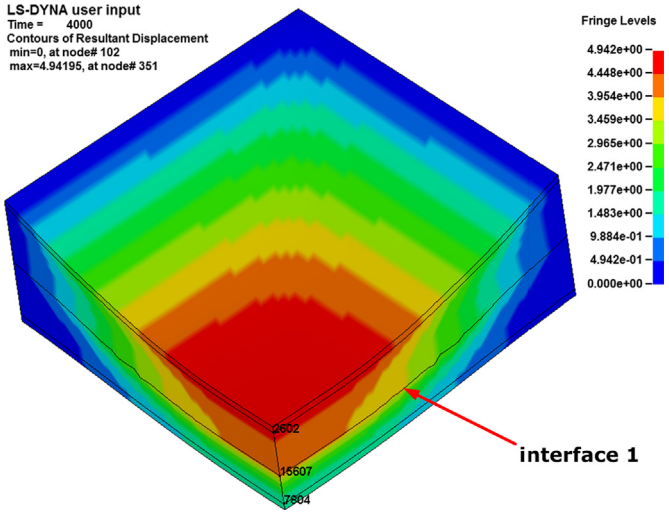

Fig. 10. Blast-induced deformation of graded sandwich plate (configuration 4) with perfect connection.

example, is calculated from the difference between the transverse displacements of top face-sheet and interface 1. By comparing the initial slopes of the normalized transverse deflection versus time curves, it is evident that the bottom face-sheet moves at the slowest speed down from the air blast loading, due to the need to communicate the movement of the top face-sheet through the dynamically crushing foam core. In contrast, the deformation of the top face-sheet increases at the fastest pace as a result of its proximity to the blast source, whilst the deformation speed of interface 1 lies in between the top and bottom face-sheets. Simultaneously, the bottom face-sheet possesses the minimal normalized permanent transverse deflection (0.074), much less than that (0.198) of the top face-sheet. Due to foam damping effects, it is seen from Fig. 11a that the dynamic deformation of each sandwich constituent exhibits little or few oscillations during the whole blast event.

From Fig. 11a it can be seen that the top foam layer (F6 with 19.7% relative density) is crushing less than that of bottom foam layer (F1 with 10% relative density), reaching its normalized crushing plateau of 0.037 at the normalized time of 0.22. On the other hand, the bottom foam layer completes crushing at the much delayed time of 0.46, due to its farther distance from the blast source and less impact loading sustained. For comparison, Fig. 11b plots the normalized transverse deflection of both the top and bottom face-sheets as well as the normalized core crushing as functions of time for a conventional foam-cored sandwich plate (configuration 1). As before, the compression capability of

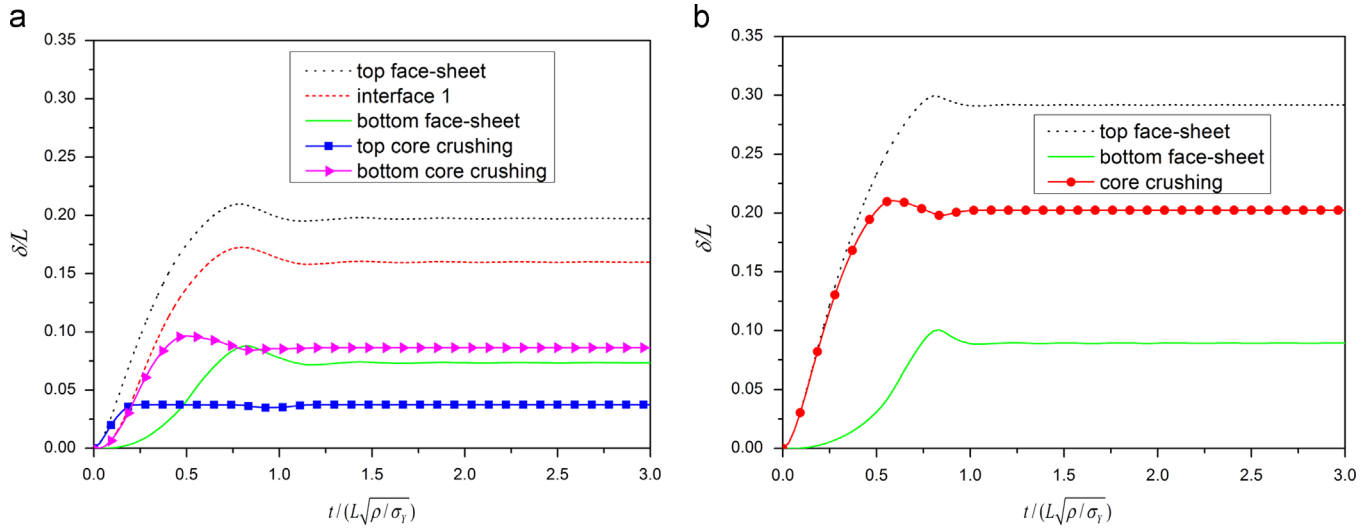

Fig. 11. Simulated time history of normalized transverse deflection and normalized foam core crushing for: (a) graded (configuration 4) and (b) conventional (configuration 1) sandwich plates with perfect connection.

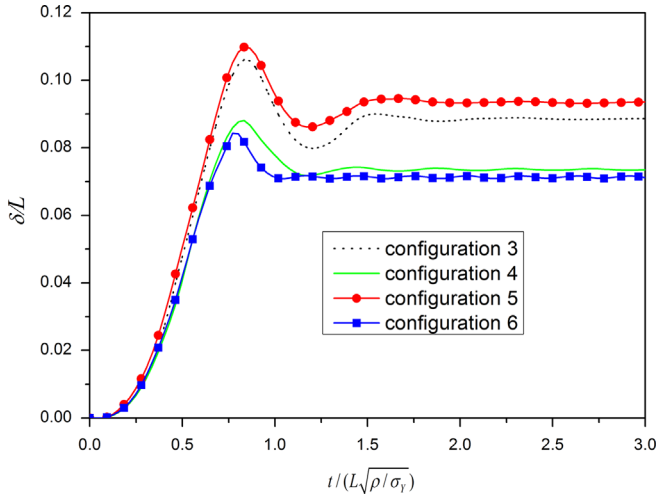

Fig. 12. Evolution of normalized transverse deflection of bottom face-sheet of graded sandwich plates having perfect connection.

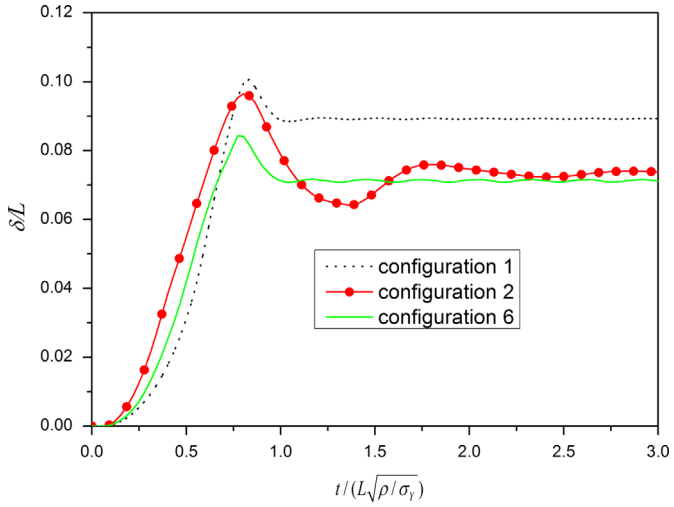

Fig. 13. Comparison of normalized transverse deflection (bottom face-sheet) between conventional and graded sandwich plates having perfect connection.

aluminum foam core (F1) reduces considerably the transverse deflection of the bottom face-sheet.

There exist several possible criteria for estimating the performance of a blast resisting sandwich structure. As the sandwich plate must protect people or objects located on the other side of the blast loading, one common way to assess its blast resistance is to examine the transverse deflection of its bottom face-sheet. For graded sandwich plates having different configurations (3–6), Fig. 12 compares the normalized transverse deflections of their bottom face-sheets when subjected to identical air blast loading. The dynamic response of the bottom face-sheet is represented by the slight oscillations occurring after the initially increasing process, which is eventually brought to rest after spring back. Configuration 5 (F1/F2/F3/F4/F5/F6) possesses the largest normalized peak transverse deflection (0.11) at the normalized time of 0.83, about 31% bigger than that achieved by configuration 6 (F6/F5/F4/F3/F2/F1), the latter also being the smallest (0.084) reached at time 0.77. Simultaneously, the permanent deflection of configuration 5 is 0.094, 32.4% larger than configurations 6. Both the peak deflection and the permanent deflection suggest that configuration 6 offers the best blast resistance amongst the four graded configurations considered. This is in conformity with the result of Ajdari et al. [36], which takes the energy absorption as the evaluation criterion. These numerical results demonstrate that a graded sandwich plate exhibits different blast responses by simply changing the arrangement of its graded foam core. It should be pointed out that the peak deflection is more important than permanent deflection because the former represents the real protection performance during the blast loading process.

As shown in Fig. 12, the blast performance of configuration 4 (F6/F1) is similar to configuration 6, because both configurations 4 and 6 have decreasing foam relative density from the loaded side to the other side. Further, both configurations 4 and 6 set F1 foam layer having the best compression capability as the bottom layer, reducing therefore the transverse deflection of the bottom face. On the contrary, configurations 3 (F1/F6) and 5 (F1/F2/F3/F4/F5/F6) both set F6 foam layer as the bottom layer, which is the hardest to compress, resulting in relatively large transverse deflection of the bottom face. Upon comparing configurations 4 and 6, it can be seen from Fig. 12 that increasing the layer number of graded foam core (configuration 6) can enhance the blast resistance of the graded sandwich plate. It should nonetheless be noted that the choice of gradation is important for the graded sandwich plate,

because a bad gradation such as configuration 5 leads to the worst blast resistance amongst the four graded sandwich plates investigated here, even though the number of its graded foam core layers is three times that of configurations 3 and 4.

Because configuration 6 exhibits the smallest transverse deformation, the time history of its normalized transverse deflection is compared with two conventional sandwich plates, as shown in Fig. 13. Configuration 2 reaches normalized peak transverse deflection (0.096) at time 0.8, about 14.3% bigger than that achieved by configuration 6 which is also the smallest (0.084) at time 0.77. The mass of the three sandwich plates differ due to different foam cores, with 26.2 kg, 32.1 kg and 29.3 kg for configurations 1, 2 and 6, respectively, and configuration 2 is about 9.6% heavier than configuration 6. These results confirm further that configuration 6 has the best blast resistance amongst the six graded and conventional sandwich plates investigated here. It may therefore be concluded that graded sandwich plates have advantage over its conventional counterparts in blast protection. Besides, configuration 2 (F6) exhibits significant oscillations because of its relatively large elastic modulus. For the two conventional sandwich plates (configurations 1 and 2), both the peak deflection and the permanent deflection decrease as the relative density of the foam core is increased.

4.2. Responses of sandwich plates with disjointed connection

The final deformed configuration of a conventional sandwich plate (configuration 1) with disjointed connection is presented in Fig. 14a, with the largest transverse deflection occurring at its central region. To present the maximum transverse deflection of the plate, four representative nodes located separately at the center of the top face-sheet (node 2602), the bottom face-sheet (node 7805), the top core face (node 15,608) and the bottom core face (node 18,208) are selected. The top face-sheet and the top core face constitute the top interface, whilst the bottom interface is composed of the bottom face-sheet and the bottom core face. Fig. 14b presents the temporal variation of normalized transverse deflection, normalized foam core crushing and normalized delamination in each constituent of configuration 1. It is clear that the normalized transverse deflection of the top face-sheet is smaller than that of the top core face, implying that delamination occurs at the top interface (as visually shown in Fig. 14a). The delamination occurs at a normalized time of 0.75, with a normalized final delamination quantity of 0.027. Similar delamination also exists at the bottom interface, happening at time 1.36, much later than that of the top interface, and the corresponding delamination quantity is 0.013. Foam core crushing is defined as the difference between the transverse displacements of two adjacent nodes at the top core face and the bottom core face, as shown in Fig. 14a. It is seen from Fig. 14b that foam core crushing reaches its normalized plateau of 0.216 at approximately time 0.59.

Fig. 15 compares the normalized transverse deflections of two conventional sandwich plates and four graded sandwich plates, each having disjointed connection. The results show that the two conventional sandwich plates have the best performance whilst the two six-layer graded sandwich plates have the worst performance. Upon increasing the foam layer number, the number of disjointed interfaces in the sandwich plate increase, reducing its blast resistance due mainly to interfacial delamination. Given that the six-layer graded sandwich plate with perfect connection (configuration 6) possesses the best blast resistance as discussed in Section 4.1, this indicates that the connection type has great effect on the dynamic response of the sandwich plate. To explore the issue further, the influence of connection type upon the

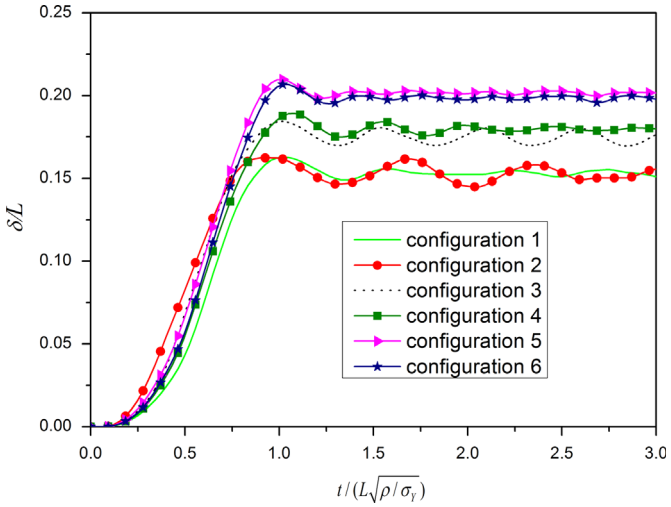

Fig. 15. Comparison of normalized transverse deflections (bottom face-sheet) of conventional and graded sandwich plates having disjointed connection.

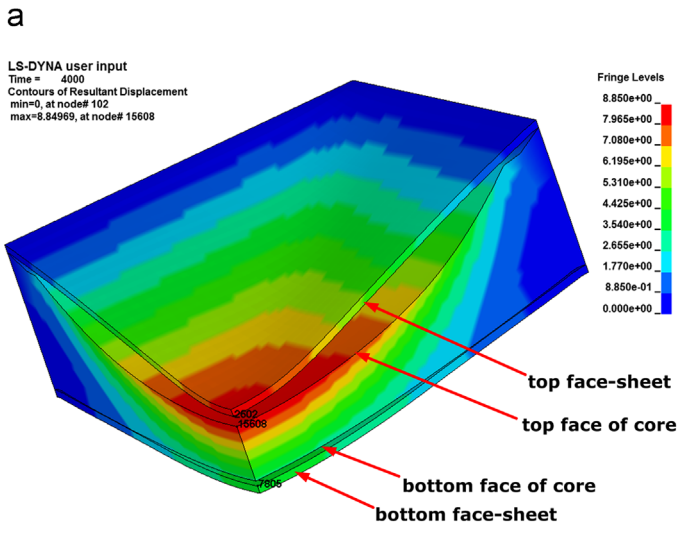

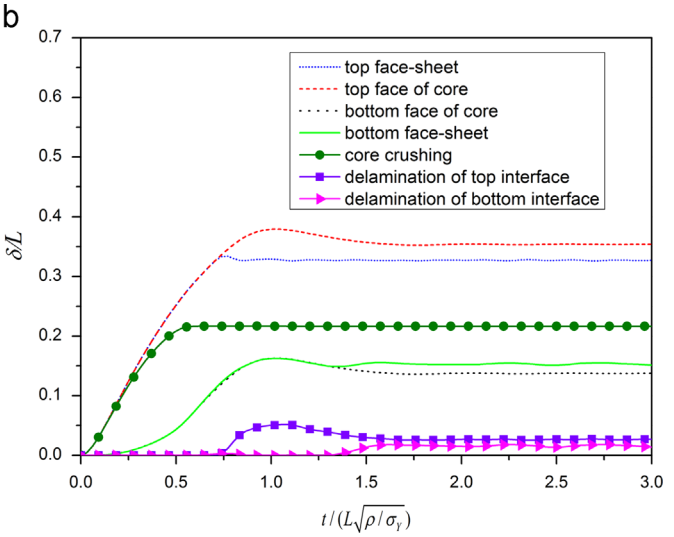

Fig. 14. (a) Final deformation of conventional sandwich plate (configuration 1) having disjointed connection (representative node number at bottom core face not shown for better view); (b) corresponding time history of normalized transverse deflection, normalized foam core crushing and normalized delamination.

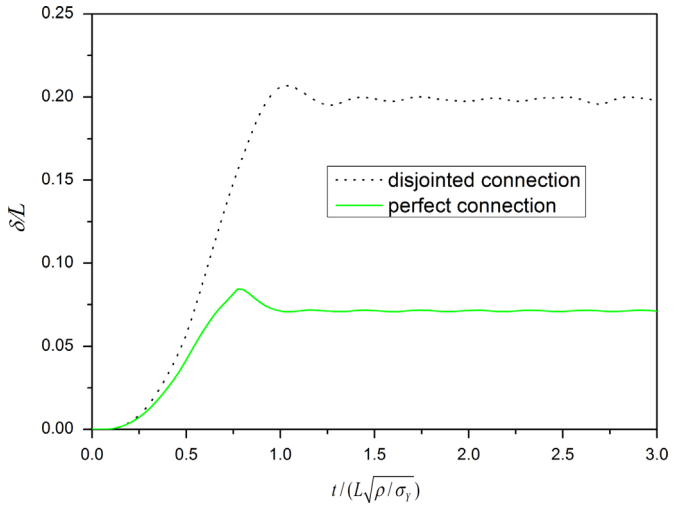

Fig. 16. Influence of connection type upon normalized transverse deflection of bottom face-sheet of graded sandwich plate (configuration 6).

Table 3
Specifications of face-sheet arrangement (total thickness fixed at 10 mm).

Face-sheet arrangement	Thickness of top face-sheet h_{ft} (mm)	Thickness of bottom face-sheet h_{fb} (mm)
FS1	1	9
FS2	3	7
FS3	5	5
FS4	7	3
FS5	9	1

normalized transverse deflection of configuration 6 is plotted in Fig. 16. Perfect connection leads to significantly smaller normalized permanent transverse deflection (0.071), only 35.7% of that achieved by disjointed connection (0.199). Similar results are found for other five sandwich plates. These findings demonstrate that, to fully utilize the performance of aluminum foam-cored sandwich plates, each component of the sandwich should be glued together and each interface should maintain certain joint strength.

5. Influence of face-sheet arrangements

To quantify the influence of face-sheet arrangement (denoted below as FS) on the blast resistance of foam-cored sandwich plates, five different face-sheet arrangements (from FS1 to FS5) with perfect connection are considered, with the total thickness of the top face-sheet and bottom face-sheet fixed at 10 mm; see Table 3. Varying from FS1 to FS5, the thickness of the top face-sheet increases whilst that of the bottom face-sheet decreases. As for the graded foam core arrangement, the two-layered configuration 4 having perfect connection (Fig. 7) is selected for simplicity.

The predicted influence of face-sheet arrangement upon the normalized transverse deflection of the bottom face-sheet is presented in Fig. 17 for sandwich configuration 4. The results of Fig. 17 show that face-sheet arrangement affects significantly the blast resistance of the sandwich. Subjected to the constraint of equivalent volume and mass, enhanced blast resistance can be achieved by simply altering the face-sheet arrangement. Amongst the five different arrangements (Table 3), FS5 has the maximal peak deflection of 0.134, with a corresponding permanent deflection of 0.122, whilst FS2 has the minimal peak deflection of 0.083, with the corresponding permanent deflection of 0.072. By simply switching the top and bottom face-sheets, it is seen from Fig. 17 that FS1 (or FS2) results in significantly smaller deflection than FS5 (or FS4). This suggests that a thicker bottom face-sheet has advantage relative to a thinner one, because the thicker bottom face-sheet renders more support and constraint for the sandwich plate. Simultaneously, it is evident that FS3 with identical top and bottom face-sheets is not the best choice, as the arrangement of thinner top face-sheet and thicker bottom face-sheet is a better sandwich design.

With the total mass (thickness) fixed, how to assign the mass (thickness) between the top and bottom face-sheets poses an interesting optimization problem. For the five arrangements considered here, FS2 appears to be the best choice (Fig. 17), suggesting that the good face-sheet arrangement is weak (thinner) top face-sheet and strong (thicker) bottom face-sheet. The results of Fig. 12 show nonetheless that the two-layer graded configuration 4 with strong top foam core (F6) and weak bottom foam core (F1) offers considerably better blast resistance than F1/F6 arrangement (configuration 3). This paradox may be attributed to the different dominant deformation modes between the foam core (crushing) and the face-sheets (bending/stretching). Fig. 18 illustrates the final total core crushing of configurations 3 and 4 that have identical top/bottom face-sheets along the X direction. The total core crushing is calculated from the difference between the transverse displacements of the top face-sheet and the bottom face-sheet. Core crushing of configuration 4 is smaller than configuration 3, implying that the sandwich plate of configuration 4 is thicker than configuration 3 after compression. In other words, configuration 4 has better bending resistance and smaller transverse deflection than configuration 3, as shown in Fig. 12. Sandwich plates with different face-sheet arrangements offer different foam core compression conditions. As the foam core is compressed, a weak (thinner) bottom face-sheet provides less support and constraint than a strong (thicker) bottom face-sheet, and hence the former induces larger transverse deflection than the latter (Fig. 17).

6. Blast resistance of sandwich plates with equivalent mass

In the analysis presented in Section 4, the conventional and graded sandwich plates have identical volume (total sandwich thickness H fixed; see Fig. 7), but different masses: whilst the four graded sandwich plates have the same mass of 29.3 kg (to be exact, the mass of configurations 3 and 4 is 29.2 kg whilst the mass of configurations 5 and 6 is 29.3 kg), the mass of the two conventional sandwich plates (26.2 kg and 32.1 kg) is considerably different. In this section, the constraint of equivalent mass is taken into account to investigate the blast resistance of sandwich plates with perfect connection. Because configuration 6 has the best performance amongst the four graded sandwich plates (see Fig. 12), it is selected to compare with the two conventional sandwich plates (configurations 1 and 2). Accordingly, on the basis of equivalent mass, the total thickness H of configuration 1, 2 and 6 are 145.6 mm, 78.8 mm and 100 mm, respectively. The normalized transverse deflections of these sandwich plates are plotted in Fig. 19, which are compared with those of Fig. 13 calculated on the basis of equivalent volume.

The results of Fig. 19 demonstrate that configuration 1 has the minimal peak and permanent transverse deflections whilst configuration 2 has the maximal values. The normalized peak transverse deflection (0.069) of configuration 1 is 17.9% smaller than that achieved by configuration 6 (0.084), but this is penalized by the much larger volume of the former: configuration 1 is 45.6% thicker than configuration 6. Consequently, it may be concluded that the graded sandwich design of configuration 6 has advantage

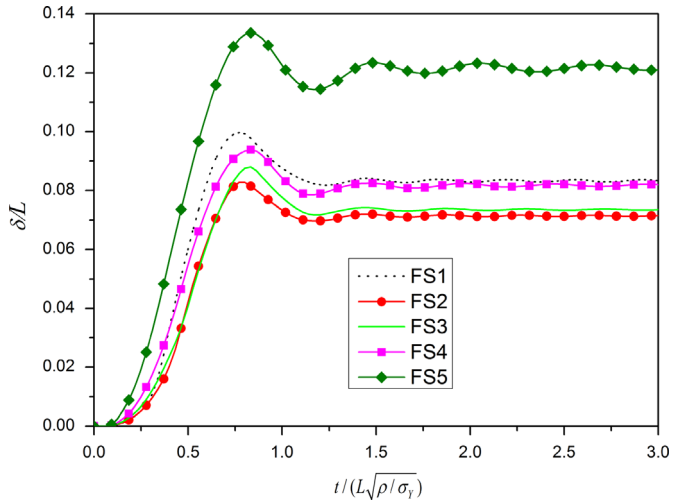

Fig. 17. Influence of face-sheet arrangement upon normalized transverse deflection (bottom face-sheet) of configuration 4 with perfect connection.

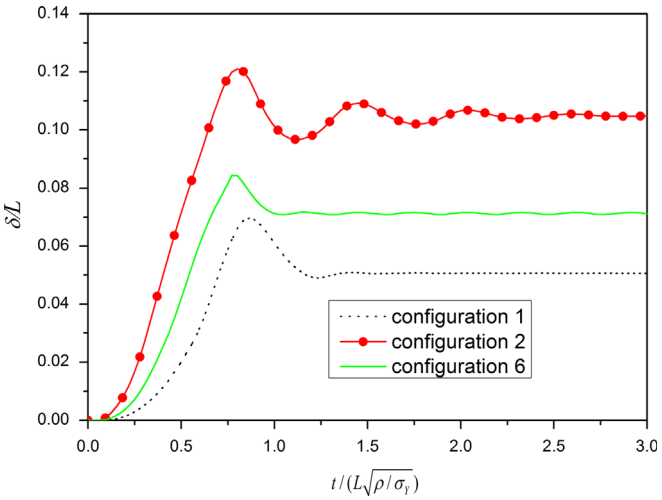

Fig. 19. Comparison of normalized transverse deflections (bottom face-sheet) of conventional and graded sandwich plates having equivalent mass and perfect connection.

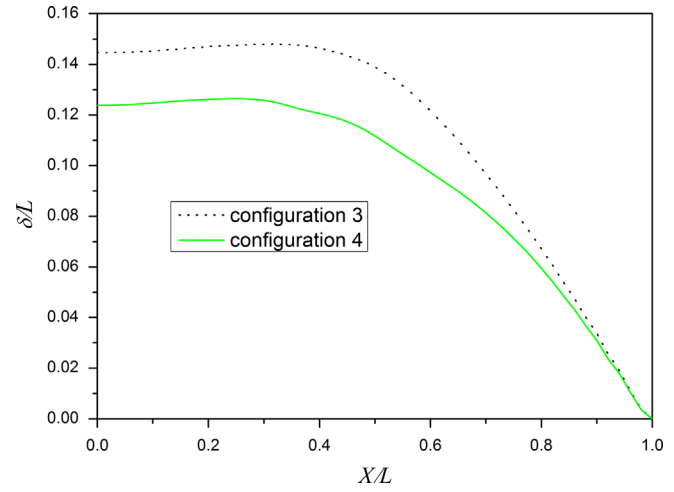

Fig. 18. Normalized total core crushing (X direction) of sandwich plates with the two-layer graded aluminum foam core having identical top/bottom face-sheets and perfect connection.

over conventional single-layer sandwich design, especially when the issue of space is acute such as road vehicles threatened by land mines.

7. Concluding remarks

The dynamic performance and blast resistance of all-metallic sandwich plates with graded aluminum foam cores are numerically simulated and compared with those of conventional (ungraded) sandwich plates. The influences of simulated blast loading type, interfacial connection condition in the sandwich and face-sheet arrangement are quantified. Existing experimental measurements for both conventional sandwich plates and monolithic plates are used to validate the numerical approach, with good agreement achieved using the exponential type of simulated pressure history. The following conclusions are drawn:

(a) Poor bonding (disjointed connection) causes large-scale interfacial delamination, resulting in larger transverse deflection of graded sandwich plates than that of conventional single-layer counterparts. To fully utilize the blast resistance capability of a graded sandwich plate, each of its interfaces should maintain certain joint strength.

(b) For perfect joint connection, configuration 6 having decreasing foam relative density from the loaded side achieves the best blast resistance amongst the various graded sandwich plates investigated, and has better performance than its conventional counterparts in terms of transverse deformation (both peak and permanent).

(c) Under the constraint of fixed total face-sheet thickness, the arrangement of thinner top face-sheet and thicker bottom face-sheet is beneficial for sandwich plate design.

(d) Concerning the blast resistance of sandwich plates with equivalent mass, the graded sandwich plate of configuration 6 has advantage over conventional sandwich plates.

Acknowledgments

This work is supported by the National Basic Research Program of China (2011CB610305), the National Natural Science Foundation of China (11072188, 11021202 and 50975221), Specialized Research Fund for the Doctoral Program of Higher Education of China (20110201110062), Science & Technology Projects of Shaanxi (2010K10-10), and Fundamental Research Funds for Central Universities.

References

[1] Fleck NA, Deshpande VS. The resistance of clamped sandwich beams to shock loading. J Appl Mech—Trans Asme 2004;71(3):386–401.
[2] Hutchinson JW, Xue ZY. Metal sandwich plates optimized for pressure impulses. Int J Mech Sci 2005;47(4-5):545–69.
[3] McShane GJ, Deshpande VS, Fleck NA. The underwater blast resistance of metallic sandwich beams with prismatic lattice cores. J Appl Mech—Trans Asme 2007;74(2):352–64.
[4] Qiu X, Deshpande VS, Fleck NA. Finite element analysis of the dynamic response of clamped sandwich beams subject to shock loading. Eur J Mech A—Solids 2003;22(6):801–14.
[5] Qiu X, Deshpande VS, Fleck NA. Dynamic response of a clamped circular sandwich plate subject to shock loading. J Appl Mech—Trans Asme 2004;71 (5):637–45.
[6] Qiu X, Deshpande VS, Fleck NA. Impulsive loading of clamped monolithic and sandwich beams over a central patch. J Mech Phys Solids 2005;53(5):1015–46.
[7] Vaziri A, Hutchinson JW. Metal sandwich plates subject to intense air shocks. Int J Solids Struct 2007;44(6):2021–35.
[8] Xue ZY, Hutchinson JW. Preliminary assessment of sandwich plates subject to blast loads. Int J Mech Sci 2003;45(4):687–705.

[9] Xue ZY, Hutchinson JW. A comparative study of impulse-resistant metal sandwich plates. Int J Impact Eng 2004;30(10):1283–305.
[10] Dharmasena KP, Wadley HNG, Xue ZY, Hutchinson JW. Mechanical response of metallic honeycomb sandwich panel structures to high-intensity dynamic loading. Int J Impact Eng 2008;35(9):1063–74.
[11] Dharmasena KP, Queheillalt DT, Wadley HNG, Chen YC, Dudt P, Knight D, et al. Dynamic response of a multilayer prismatic structure to impulsive loads incident from water. Int J Impact Eng 2009;36(4):632–43.
[12] Dharmasena KP, Queheillalt DT, Wadley HNG, Dudt P, Chen YC, Knight D, et al. Dynamic compression of metallic sandwich structures during planar impulsive loading in water. Eur J Mech A—Solids 2010;29(1):56–67.
[13] Dharmasena KP, Wadley HNG, Williams K, Xue ZY, Hutchinson JW. Response of metallic pyramidal lattice core sandwich panels to high intensity impulsive loading in air. Int J Impact Eng 2011;38(5):275–89.
[14] Wadley HNG, Dharmasena KP, Chen YC, Dudt P, Knight D, Charette R, et al. Compressive response of multilayered pyramidal lattices during underwater shock loading. Int J Impact Eng 2008;35(9):1102–14.
[15] Wei Z, Dharmasena KP, Wadley HNG, Evans AG. Analysis and interpretation of a test for characterizing the response of sandwich panels to water blast. Int J Impact Eng 2007;34(10):1602–18.
[16] Wei Z, Deshpande VS, Evans AG, Dharmasena KP, Queheillalt DT, Wadley HNG, et al. The resistance of metallic plates to localized impulse. J Mech Phys Solids 2008;56(5):2074–91.
[17] Radford DD, Deshpande VS, Fleck NA. The use of metal foam projectiles to simulate shock loading on a structure. Int J Impact Eng 2005;31:1152–71.
[18] Radford DD, Fleck NA, Deshpande VS. The response of clamped sandwich beams subjected to shock loading. Int J Impact Eng 2006;32:968–87.
[19] Radford DD, McShane GJ, Deshpande VS, Fleck NA. The response of clamped sandwich plates with metallic foam cores to simulated blast loading. Int J Solids Struct 2006;43:2243–59.
[20] McShane GJ, Radford DD, Deshpande VS, Fleck NA. The response of clamped sandwich plates with lattice cores subjected to shock loading. Eur J Mech A—Solids 2006;25:215–29.
[21] Tagarielli VL, Deshpande VS, Fleck NA. The dynamic response of composite sandwich beams to transverse impact. Int J Solids Struct 2007;44:2442–57.
[22] Bahei-El-Din YA, Dvorak GJ, Fredricksen OJ. A blast-tolerant sandwich plate design with a polyurea interlayer. Int J Solids Struct 2006;43:7644–58.
[23] Zhu F, Zhao LM, Lu GX, Wang ZH. Structural response and energy absorption of sandwich panels with an aluminium foam core under blast loading. Adv Struct Eng 2008;11(5):525–36.
[24] Zhu F, Zhao LM, Lu GX, Wang ZH. Deformation and failure of blast-loaded metallic sandwich panels—experimental investigations. Int J Impact Eng 2008;35(8):937–51.
[25] Zhu F, Zhao LM, Lu GX, Gad E. A numerical simulation of the blast impact of square metallic sandwich panels. Int J Impact Eng 2009;36(5):687–99.
[26] Nurick GN, Langdon GS, Chi Y, Jacob N. Behaviour of sandwich panels subjected to intense air blast—part 1: experiments. Compos Struct 2009;91(4):433–41.
[27] Karagiozova D, Nurick GN, Langdon GS. Behaviour of sandwich panels subject to intense air blasts—part 2: numerical simulation. Compos Struct 2009;91(4):442–50.
[28] Theobald MD, Langdon GS, Nurick GN, Pillay S, Heyns A, Merrett RP. Large inelastic response of unbonded metallic foam and honeycomb core sandwich panels to blast loading. Compos Struct 2010;92(10):2465–75.
[29] Shen JH, Lu GX, Wang ZH, Zhao LM. Experiments on curved sandwich panels under blast loading. Int J Impact Eng 2010;37(9):960–70.
[30] Li Y, Ramesh KT, Chin ESC. Dynamic characterization of layered and graded structures under impulsive loading. Int J Solids Struct 2001;38(34-35):6045–61.
[31] Apetre NA, Sankar BV, Ambur DR. Low-velocity impact response of sandwich beams with functionally graded core. Int J Solids Struct 2006;43(9):2479–96.
[32] Etemadi E, Khatibi AA, Takaffoli M. 3D finite element simulation of sandwich panels with a functionally graded core subjected to low velocity impact. Compos Struct 2009;89(1):28–34.
[33] Wang EH, Gardner N, Shukla A. The blast resistance of sandwich composites with stepwise graded cores. Int J Solids Struct 2009;46(18 and 19):3492–502.
[34] Chittineni K, Woldesenbet E. Characterization of integrated functionally gradient syntactic foams. J Eng Mater Technol—Trans Asme 2010;132:1.
[35] Gunes R, Aydin M. Elastic response of functionally graded circular plates under a drop-weight. Compos Struct 2010;92(10):2445–56.
[36] Ajdari A, Nayeb-Hashemi H, Vaziri A. Dynamic crushing and energy absorption of regular, irregular and functionally graded cellular structures. Int J Solids Struct 2011;48:506–16.
[37] Gardner N, Wang E, Shukla A. Performance of functionally graded sandwich composite beams under shock wave loading. Compos Struct 2012;94:1755–70.
[38] Zhang J, Zhao GP, Lu TJ. Experimental and numerical study on strain rate effects of close-celled aluminum foams. J Xi'an Jiaotong Univ 2010;44(5):97–101.
[39] Zhang J, Zhao GP, Lu TJ. Dynamic responses of sandwich beams with gradient-density aluminum foam cores. Int J Prot Struct 2011;2(4):439–51.
[40] Liu XR, Tian XG, Lu TJ, Zhou D, Liang B. Blast resistance of sandwich-walled hollow cylinders with graded metallic foam cores. Compos Struct 2012;94(8):2485–93.